Published in final edited form as:
J Cell Biochem. 2011 August ; 112(8): 2149–2159. doi:10.1002/jcb.23136.

Myogenin Regulates Denervation-Dependent Muscle Atrophy in Mouse Soleus Muscle

Peter C. D. Macpherson[*], **Xun Wang**[*], and **Daniel Goldman**
Molecular and Behavioral Neuroscience Institute and Department of Biological Chemistry, University of Michigan, Ann Arbor, MI 48109

Abstract

Muscle inactivity due to injury or disease results in muscle atrophy. The molecular mechanisms contributing to muscle atrophy are poorly understood. However, it is clear that expression of atrophy-related genes, like Atrogin-1 and MuRF-1, are intimately tied to loss of muscle mass. When these atrophy-related genes are knocked out, inactive muscles retain mass. Muscle denervation stimulates muscle atrophy and Myogenin (Myog) is a muscle-specific transcription factor that is highly induced following muscle denervation. To investigate if Myog contributes to muscle atrophy, we have taken advantage of conditional Myog null mice. We show that in the denervated soleus muscle Myog expression contributes to reduced muscle force, mass and cross sectional area. We found that Myog mediates these effects, at least in part, by regulating expression of the *Atrogin-1* and *MuRF-1* genes. Indeed Myog over-expression in innervated muscle stimulates *Atrogin-1* gene expression and Myog over-expression stimulates *Atrogin-1* promoter activity. Thus Myog and the signaling cascades regulating its induction following muscle denervation may represent novel targets for therapies aimed at reducing denervation-induced muscle atrophy.

Keywords

Myogenin; Atrogin-1; MuRF-1; muscle mass; muscle force; muscle cross sectional area; muscle denervation

Introduction

Disease and injury of the neuromuscular system often results in lost muscle activity which leads to muscle atrophy. This atrophy is a consequence of catabolism of muscle proteins. Although muscle catabolism can be beneficial in times of need, its long term consequences can be dire. Interestingly, not all muscles atrophy to the same extent in response to inactivity. Muscles enriched with slow fiber types, such as the soleus muscle, atrophy to a greater extent than those with predominantly fast fiber-types [Grossman et al., 1998]. During soleus muscle atrophy, slow fiber-type myosin heavy chain isoforms are lost, while faster type II isoforms are increased [Grossman et al., 1998].

One approach for identifying ways of preventing or reversing the detrimental consequences of muscle atrophy is to identify mechanisms underlying this process. It is hoped that these mechanisms may suggest novel strategies for intervention. In general, muscle atrophy is accompanied by activation of the ubiquitin-proteosome system [Cao et al., 2005; Ventadour

Corresponding Author Daniel Goldman, University of Michigan, 5045 BSRB, 109 Zina Pitcher Place, Ann Arbor, MI 48109, neuroman@umich.edu, Phone: 734-936-2057, Fax: 734-936-2690.
[*]These authors contributed equally to this work.

and Attaix, 2006]. In this system proteins are targeted for degradation by being polyubiquinated and then degraded by the 26S proteosome. Two ubiquitin-protein ligases, Atrogin-1 (Fbxo32/MAFbx) and MuRF-1 (Trim63), are induced in atrophying skeletal muscle and knockout mice lacking either of these ligases exhibit reduced denervation-dependent muscle atrophy [Bodine et al., 2001a; Gomes et al., 2001]. Although muscle atrophy is most dramatic around 2–4 weeks following muscle denervation, the expression of *Atrogin-1* and *MuRF-1* transcripts peak around 3 days post-denervation when the rate of muscle weight loss is most rapid [Sacheck et al., 2007].

A number of studies have shown that activation of the IGF-1/PI3K/AKT signaling pathway can stimulate muscle hypertrophy and inhibition of this pathway can lead to muscle atrophy [Bodine et al., 2001b; Rommel et al., 2001; Stitt et al., 2004]. This pathway was also shown to regulate *Atrogin-1* expression via phosphorylation of FoxO transcription factors [Sandri et al., 2006; Sandri et al., 2004]. In addition, denervation-dependent suppression of PGC-1α (peroxisome proliferator-activated receptor γ-coactivator 1α) expression stimulates muscle atrophy by relieving repression of Atrogin-1 expression [Sandri et al., 2006]. Finally, cytokines, such as TNF-like weak inducer of apoptosis (TWEAK), can stimulate muscle atrophy via a NF-kB signaling pathway that regulates MuRF-1 expression [Mittal et al., 2010].

We reasoned that muscle-specific transcription factors that are also regulated in an activity-dependent manner may be good candidates for regulating genes, like *Atrogin-1* and *MuRF-1*, which stimulate muscle atrophy. One such gene encodes Myogenin (Myog), a basic helix-loop-helix transcription factor that is necessary for muscle differentiation and is regulated by muscle activity [Eftimie et al., 1991; Hasty et al., 1993]. Indeed, while this manuscript was in preparation, it was reported that Myog contributes to denervation-dependent muscle atrophy by controlling expression of atrophy-related genes like *MuRF-1* and *Atrogin-1* [Moresi et al., 2010]. However these studies were confined to relatively fast muscles and did not investigate if Myog also regulates atrophy of slow muscles. Furthermore these previous studies did not investigate if any of the consequences of muscle denervation and *Myog* deletion were a result of compensation by the contralateral innervated muscle or due to increase satellite cell proliferation and fusion.

Here we report that Myog contributes to denervation-dependent atrophy of the slow soleus muscle via regulated expression of *Atrogin-1* and *MuRF-1* gene expression. We demonstrate that this effect is intrinsic to the denervated hindlimb and not a result of compensation by the contralateral limb or by increased myoblast proliferation and fusion in the *Myog* null denervated muscle. Our data suggest that denervation-induced muscle atrophy, and its regulation by Myog, is more dramatic in the predominantly slow soleus muscle compared to the fast EDL muscle. We go on to show that attenuation of muscle atrophy by Myog is also reflected in muscle function (force generation). Finally consistent with the idea that Myog directly regulates *Atrogin-1* and *MuRF-1* gene expression, we show that all 3 genes are coordinately suppressed by muscle electrical activity and that distal E-boxes in the *Atrogin-1* promoter are most effective in mediating Myog-dependent promoter regulation. These data, along with those of Moresi et al., 2010, suggest Myog induction in denervated muscle contributes to the development of muscle atrophy via regulated expression of ubiquitin ligases Atrogin-1 and Murf-1.

Materials and Methods

Animals and tamoxifen-induced recombination

All animal studies were approved by the University of Michigan Committee on Use and Care of Animals. Myog conditional knockout mice (*Myog*$^{flox/flox}$*;CAGG-CreER*^{TM}) were

described previously [Knapp et al., 2006]. To induce recombination in Myog conditional knockout mice, 1 mg of tamoxifen suspended in sunflower seed oil was injected intraperitoneally into adult mice for five consecutive days followed by a 2 day rest and then repeated. Tamoxifen-induced recombination should result in deletion of exon 1 in the *Myog* gene [Knapp et al., 2006]. *Myog* exon 1 deletion was confirmed by PCR using genomic DNA isolated from extensor digitorum longus (EDL) muscles of *Wt* (wild type) and *Myog$^{flox/flox}$;CAGG-CreER*™ tamoxifen injected mice. EDL muscles were dissected, lysed in 100 μl of 25 mM NaOH, 0.2 mM EDTA at 95° C for 20 minutes and then buffered by addition of an equal volume of 40mM Tris-HCl (pH 7.8). Samples were vortexed briefly and centrifuged at 2000 rpm for 10 min. One microliter of lysed muscle containing genomic DNA was used for each PCR reaction. To test for tamoxifen-induce recombination, primers were designed to amplify a genomic DNA fragment spanning the majority of exon 1 (forward primer 5′CTACCAGGAGCCCCACTTCTATGATG) and a portion of exon 2 (reverse primer 5′AGGAGGCGCTGTGGGAGTTGC). Amplification of genomic γ-actin DNA was performed with forward 5′AGAAGAAATCGCCGCACTCGTCAT and reverse 5′CCTCTTGCTCTGGGCCTCGTCAC primers and served as an internal loading control. We also confirmed the efficacy of tamoxifen-induced recombination in adult mice by assaying *Myog* mRNA in mice treated with and without tamoxifen following denervation of the tibialis anterior muscle (see below for muscle denervation protocol, satellite cell protocol, RNA isolation protocol and primers used to assay *Myog* mRNA levels).

Muscle denervation

Muscle denervation was used to induce muscle atrophy and investigate the consequences of muscle denervation on muscle function and gene expression. For muscle denervation experiments, mice were anesthetized by intraperitoneal injection of ketamine (100mg/kg) and xylazine (10mg/kg). Fur covering the lower back to proximal thigh was removed; the region was swabbed with Betadine and a small posterolateral cutaneous incision (1–2cm) was made beginning near the sciatic notch. The superficial facia was cut and the hamstring and gluteal muscles were separated bluntly to reveal the sciatic nerve. A 1 cm long region of the sciatic nerve was excised and the incision was closed with wound clips. Three to fourteen days later muscles were harvested for molecular and physiological assays.

Satellite cell proliferation in denervated muscle and cell culture

To assay satellite cell proliferation in denervated muscle, bromodeoxyuridine (BrdU, 50 mg/kg dissolved in 100 μl of 0.9% saline) was intraperitoneally injected daily, beginning at 5 days post denervation and continuing for the next 8 days. Dissected soleus muscles were embedded in OCT, frozen in liquid nitrogen, sectioned to 10 microns and fixed in 4% paraformaldehyde. Immunofluorescence was performed as previously described [Ramachandran et al., 2010], using the following primary antibodies: mouse anti-laminin B2, D18 (Developmental Studies Hybridoma Bank, University of Iowa, 1:25 dilution); rat anti-BrdU (Abcam, 1:500 dilution). Secondary antibodies were conjugated to Alexa Fluor 488 or Cy3 and used at 1:500 for anti-mouse and 1:250 for anti-rat. For BrdU detection, sections were pre-treated with 2 N HCl for 20 min at 37 °C and then soaked in 100 mM sodium borate for 10 min. Following immunohistochemical staining, slides were rinsed with water and allowed to dry in the dark before cover-slipping with 2.5% (w/v) PVA (PVA-polyvinyl alcohol)/DABCO (1,4 diazabicyclo (2.2.2)octane). Slides were examined in a Zeiss Axiophot fluorescence microscope equipped with a digital camera.

Muscle satellite cells were purified from extensor digitorum longus and soleus muscles to determine if tamoxifen-induced recombination successfully deleted the *Myog* gene in satellite cells. Muscles were isolated from innervated and 3 day denervated *Wt* and *Myog$^{flox/flox}$;CAGG-CreER*™ mice that were previously treated with tamoxifen as described

above. Dissected muscles were incubated in collagenase (0.2% w/v) at 37 °C for 1.5–2 hrs, washed 3 × with DMEM and triturated through a wide bore glass pipette that was pre-coated with horse serum and then triturated through a P1000 pipetman blue tip. Muscle fragments in 2–4 ml of DMEM were transferred to a 15 ml Falcon tube and allowed to settle for 10 min. After removing the supernatant, muscle fragments were resuspended in 7 ml of 20% fetal bovine serum, DMEM and 1 × antibiotics and distributed into tissue culture plates coated with Matrigel. The following day muscle fragments were removed, satellite cells allowed to proliferate and 3–4 days later harvested for RNA isolation and RT-PCR.

Muscle denervation and electrical stimulation

We used direct stimulation of denervated muscle with extracellular electrodes to examine if *Atrogin-1* and *MuRF-1* gene expression, like *Myog* gene expression, is regulated by muscle electrical activity. Denervation and electrical stimulation were carried out on rat soleus muscle as previously described [Goldman et al., 1988]. Briefly, the lower hind limb muscles were bilaterally denervated in anesthetized Sprague Dawley rats by removing a small segment of the sciatic nerve at mid thigh. Stimulating electrodes were implanted into one hind limb and the soleus muscle was stimulated chronically for up to 2 days in 100 Hz trains, 1 sec duration, applied once every 100 sec. Stimulus pulses within trains were of alternating polarity, their duration was 0.5 msec and their strength was 10–15 mA. At the end of the stimulation period, stimulated and contralateral unstimulated soleus muscles were excised and RNA extracted for RT-PCR.

Muscle force, fiber area and mass measurements

To investigate the consequences of muscle denervation and *Myog* deletion on muscle atrophy, muscle force, area and mass were measured. Innervated and 14 day denervated soleus and EDL muscles were isolated from adult *Wt* and tamoxifen treated *Myog* conditional knockout mice. Suture ties (5-0) were secured around the distal and proximal tendons, and the muscles were carefully removed and placed in a horizontal bath containing buffered mammalian Ringer solution (137mM NaCl, 24mM $NaHCO_3$, 11mM glucose, 5mM KCl, 2mM $CaCl_2$, 1mM $MgSO_4$, 1mM NaH_2PO_4, and 0.025mM turbocurarine chloride) maintained at 25°Cand bubbled with 95% O_2-5% CO_2 to stabilize pH at 7.4. One tendon of the muscle was tied securely to a force transducer (modelBG-50, Kulite Semiconductor Products, Leonia, NJ) and the other tendon to a fixed post.

To determine maximum isometric tetanic force (P_o), muscles were stimulated between two stainless steel plate electrodes. The voltage of single 0.2-ms square stimulation pulses and, subsequently, muscle length were adjusted to obtain maximum twitch force. The muscle length at which maximum twitch force was obtained was measured with calipers to determine the optimal length for force development (L_o). With the muscle held at L_o, the force developed during trains of stimulation pulses was recorded, and stimulation frequency was increased until the maximum isometric tetanic force (P_o) was achieved. For each muscle, optimum fiber length (L_f) was calculated by multiplying L_o by previously determined L_f/L_o ratios for EDL and soleus muscles of 0.45 and 0.71, respectively [Brooks and Faulkner, 1988]. After force measurements, muscles were removed from the bath, the tendons were trimmed, and the muscle was blotted and weighed. Muscles were quick frozen in isopentane cooled with liquid nitrogen and stored at −80°C for subsequent histological analyses. Total muscle cross-sectional area (CSA) was calculated by dividing the muscle mass by the product of L_f and the density of mammalian skeletal muscle, 1.06 g/cm^3. Changes in average muscle fiber cross-sectional areas after denervation were determined on muscle cryo-sections (14 μm) taken from the mid-region of soleus muscles. Muscle sections were stained with hematoxylin and eosin to identify the borders of individual muscle fibers and the areas of 100 fibers/muscle were determined with ImageJ (NIH). Changes in muscle

mass, P_o, total cross-sectional area and average fiber area after denervation are expressed relative to corresponding contra lateral innervated muscles (n = 4 for each condition except where identified). Differences between the experimental and *Wt* samples were assessed by a 2-tailed Student's *t* test, with the assumption of 2-sample equal variance. Values are expressed as means ± 1 SEM and significance was set *a priori* at $P < 0.05$.

In vivo muscle electroporation

We used electroporation to facilitate DNA uptake by muscle fibers in order to investigate the consequences of Myog overexpression on *Atrogin-1* and *MuRF-1* gene expression and *Atrogin-1* promoter activity. For *in vivo* Myog overexpression, 5 μg *pCS2:EGFP* plasmid (gift from D. Turner, University of Michigan, Ann Arbor) and either 20 μg of *pCS2:Myog*[Tang et al., 2001] or control empty vector (*pCS2*) were injected into innervated soleus muscles of anesthetized adult mice. For *in vivo* analysis of *Atrogin-1* promoter activity, 15μg of *pCS2:Myog* or *pCS2* along with 5μg of *pCS2:EGFP*, 5 μg of the *Atrogin-1:luciferase* reporter plasmid [Sandri et al., 2004] and 5 μg of the normalization vector, *ubC:Renilla* luciferase (gift from M. Uhler, University of Michigan, Ann Arbor), were injected into left and right hindlimb innervated EDL or soleus muscles. Plasmid uptake was facilitated by placing square flat stainless steel electrodes, coated with ultrasound transmission gel, on each side of the leg and using a BTX840 square wave electroporator to deliver 8 pulses of 140V/cm of 60-ms duration with an interval of 100ms. Mice were allowed to recover 12 days before isolation of electroporated GFP^+ fibers (for Myog over-expression in innervated muscle) or before denervation (for *Atrogin-1* promoter analysis). Electroporated GFP^+ were identified under a stereomicroscope (Leica MZFLIII) equipped with fluorescence optics. GFP^+ fibers were dissected in ice-cold phosphate-buffered saline (PBS) and then immediately lysed for RNA and luciferase assays. All experiments were performed in triplicate and results are expressed as mean ± SEM. RNA levels were assayed by RT-PCR using the following primers: *γ-Actin* forward 5′CCAGGCATTGCTGACAGGATGC and reverse 5′GTCCATCTAGAAGCATTTGCGGTGGACG; *Myog* forward 5′GAGAAGCACCCTGCTCAAC and reverse 5′GGTGACAGACATATCCTCC; *Atrogin-1* forward 5′GTCCAGAGAGTCGGCAAGTC and reverse 5′GTAGCCGGTCTTCACTGAGC and *MuRF-1* forward 5′GAGAACCTGGAGAAGCAGCT and reverse 5′CCGCGGTTGGTCCAGTAG.

RNA isolation and Real-time PCR

Total RNA was isolated using TRIzol (Invitrogen). The Turbo DNase Kit (Ambion) was used to remove residual DNA and total RNA was quantified spectrophotometrically. One microgram of total RNA was used to generated cDNA with oligo(dT) primers and Superscript II reverse transcriptase (Invitrogen). Real-time PCR was performed with SYBR green mix (1:20,000 SYBR green) on an iCycler iQ real-time detection system (BioRad) according to the manufacturer's instructions. Each reaction was performed in triplicate on at least three samples for each condition in a volume of 20 μl. The specificity and efficiency of the primers used in Real-time PCR were first verified by 1% agarose gel electrophoresis. PCR cycles were 95°C for 5 mins, 95°C for 30s, 58°C for 30s, and 72°C for 30s (total 40 cycles). All real-time PCR results were normalized to *γ-Actin*. The primers used are: *Myog* forward 5′-AGTGAATGCAACTCCCACAG and reverse 5′-CTGGGAAGGCAACAGACATA; *Atrogin-1* forward 5′-AACCGGGAGGCCAGCTAAAGAACA and reverse 5′-TGGGCCTACAGAACAGACAGTGC; *MuRF-1* forward 5′-GAGAACCTGGAGAAGCAGCT and reverse 5′-CCGCGGTTGGTCCAGTAG; *FoxO3* forward 5′-ATCGCCTCCTGGCGGGCTTA and reverse 5′-ACGGCGGTGCTAGCCTGAGA; *γ-actin* forward 5′-

AGAAGAAATCGCCGCACTCGTCAT and reverse 5′-CCTCTTGCTCTGGGCCTCGTCAC. Results are expressed as means ± SEM.

Western blots

Western blots were used to investigate if denervation-dependent Myog protein induction preceded denervation-dependent induction of atrophy-related genes. Western blotting was performed as previously described [Kostrominova et al., 2000]. Briefly, muscles were dissected, frozen in liquid nitrogen, pulverized and homogenized in 20 mM Tris-HCl (pH 6.8), 4% (w/v) SDS, 1 mM phenymethylsulfonyl fluoride and 1 μM each of leupeptin and pepstatin A. Protein concentration was determined using the Bio-Rad detergent compatible protein assay. Protein samples were resolved by SDS-PAGE (10%) and transferred electrophoretically to PVDF membranes. Membranes were blocked in Blotto buffer containing 5% dry milk, 0.05% Tween 20 and incubated overnight at 4 °C with mouse monoclonal anti-myogenin antibody (1:50 dilution; clone F5D, Developmental Studies Hybridoma Bank, The University of Iowa, Iowa City). Secondary antibody was goat anti-mouse HRP used at 1:200 dilution and BM chemiluminescence detection was done according to manufacturers protocol (Roche). Blots were stripped and reprobed with anti-sarcomeric myosin antibody (1:250 dilution; clone MF20, Developmental Studies Hybridoma Bank, The University of Iowa, Iowa City).

Results

Conditional *Myog* gene deletion in adult mice

We used *Myog*$^{flox/flox}$*;CAGG-CreER*™ [Knapp et al., 2006] to delete the *Myog* gene in adult animals. Tamoxifen treatment of adult *Myog*$^{flox/flox}$*;CAGG-CreER*™ mice should induce recombination of the floxed *Myog* gene and prevent *Myog* gene expression. The Myog gene contains 3 exons, and exon 1 is flanked by loxP sites in the *Myog*$^{flox/flox}$*;CAGG-CreER*™ mouse. Using PCR primers designed to amplify exon 1, we find that our regimen of tamoxifen treatment results in its deletion (Fig. 1, top panel). Because *Myog* gene expression is low in innervated muscle and highly induced following muscle denervation [Eftimie et al., 1991; Kostrominova et al., 2000; Tang and Goldman, 2006; Tang et al., 2009; Tang et al., 2006], one can also test the efficacy of tamoxifen treatment by assaying *Myog* RNA levels in innervated and denervated muscle. For this analysis we injected *Myog*$^{flox/flox}$*;CAGG-CreER*™ mice with tamoxifen or vehicle and then the left lower hindlimb muscles were denervated by cutting the sciatic nerve and 7 days later, innervated (right hindlimb) and denervated (left hindlimb) muscles were dissected and *Myog* and *γ-actin* mRNA levels assayed by RT-PCR. We found that innervated muscles of control and tamoxifen-treated mice expressed very low to undetectable levels of *Myog* mRNA (Fig. 1, bottom panel). In contrast, muscle denervation dramatically induced *Myog* expression only in control mice that did not receive tamoxifen, while *Myog* expression remained undetectable in denervated muscles of mice that received tamoxifen (Fig. 1, bottom panel). We also isolated satellite cells from innervated and denervated muscle to determine if tamoxifen treatment deleted *Myog* from satellite cells. *Myog* expression is undetectable in satellite cells isolated from innervated muscle and increased in satellite cells isolated from denervated muscle; however, following tamoxifen treatment *Myog* remains undetectable in muscle satellite cells isolated from denervated muscle (Fig. 1, middle panel).

Myog contributes to muscle mass, force and cross sectional areas.

We next deleted *Myog* in adult mice and denervated the left lower hindlimb muscles for 14 days; a similar denervation protocol was performed on *Wt* mice for comparison. During preliminary experiments we determined that 2 weeks of muscle denervation had no

significant effect on either muscle mass or maximum isometric force in the contralateral innervated soleus or EDL muscle of denervated animals when compared to muscles isolated from age and weight matched mice whose muscles remained innervated (Fig. 2A & B). Consequently, all subsequent experiments were performed making use of the contralateral innervated limb as the internal control. Fast fiber-type EDL and slow fiber-type soleus muscles were then dissected for measurements of muscle mass, force and cross-sectional area. Consistent with that reported by others [Grossman et al., 1998], we found that the slow soleus muscle atrophied to a greater extent (44% loss in muscle mass) than the fast EDL muscle (26% loss in muscle mass) (Fig. 2C). Interestingly, soleus and EDL muscle atrophy was attenuated in *Myog* knockout mice where they lost only about half as much mass as the *Wt* animals (22% loss of mass for soleus and 14% loss in mass for EDL) (Fig. 2C). Similar to muscle mass measurements, the maximum isometric force developed by denervated EDL and soleus muscles was significantly less than the contralateral innervated muscles (Fig. 2D). However, in this case there was no significant difference between *Wt* and *Myog* knockout animals in the magnitude of the force decrease in EDL muscles (approx. 20%), while in soleus muscles the decreases in maximum isometric force were much greater for *Wt* than *Myog* knockout mice (42% vs 22%, respectively) (Fig. 2D). In general, these data are consistent with the hypothesis that Myog plays a regulatory role during the development of muscle atrophy. The lack of a significant effect of *Myog* knockout on the development of maximum isometric force in EDL muscles is perplexing. We speculate that this is due, in part, to the relatively small amount of atrophy observed in the EDL muscles which limited our ability to resolve differences in force. Because of the much larger differences in both mass and maximum force development in the denervated soleus muscles of *Wt* and *Myog* knockout mice, we chose to focus our experiments on this muscle.

When mass and force values were used to deduce muscle cross-sectional areas, we also found a statistically significant attenuation of denervation-induced atrophy in the soleus muscle (Fig. 3A). To more carefully examine this, we sectioned soleus muscle from innervated and 14 day denervated *Wt* and *Myog* knockout mice and quantified fiber cross-sectional areas. Consistent with our force and mass measurements, this analysis indicated that individual fibers atrophied less in the absence of Myog (Fig. 3B). Calculations of cross-sectional areas from 100 random fibers indicated a denervation-dependent reduction in fiber cross-sectional area of 51.5 +/−3.9% in *Wt* soleus muscle and only 34 +/−3.4% reduction in soleus muscle fibers lacking Myog expression.

We next investigated if *Myog* deletion had a consequence on satellite cell proliferation and fusion with denervated muscle fibers which may account for preservation of muscle mass in *Myog* knockout animals. For these experiments we treated *Wt* and *Myog* knockout mice with BrdU after muscle denervation. Two weeks later soleus muscles were monitored for BrdU incorporation into denervated muscle fibers. Although we were able to detect scattered BrdU labeled satellite cells in the interstitial regions of *Wt* animals (~22 ±4 $BrdU^+$ cells/soleus muscle, n=3) there was no BrdU-labeled nuclei in *Myog* knockout animals (Fig. 3C). Therefore increased satellite cell proliferation and fusion cannot explain the maintenance of muscle mass in *Myog* knockout animals.

Myog, *Atrogin-1* and *MuRF-1* gene expression are coordinately regulated by muscle electrical activity

Knockout mice lacking either Atrogin-1 or MuRF-1 exhibit reduced denervation-induced muscle atrophy compared to *Wt* mice [Bodine et al., 2001a]. Therefore it is possible that Myog mediates its effects on muscle atrophy by controlling *Atrogin-1* and *MuRF-1* gene expression. Consistent with this idea, *Atrogin-1* and *MuRF-1* mRNAs, like *Myog* mRNA, are induced following muscle denervation (Fig. 4) [Bodine et al., 2001a] and *Myog* mRNA and protein induction appears to precede *Atrogin-1* and *MuRF-1* mRNA induction (Fig. 4).

Denervation dependent gene regulation can result from loss of trophic factors released from the motor neuron [Mejat et al., 2003]; however, *Myog* gene expression is largely regulated by muscle electrical activity independent of motor innervation [Buonanno et al., 1992; Eftimie et al., 1991]. Interestingly, direct stimulation of denervated rat soleus muscle with extracellular electrodes rapidly suppressed not only *Myog*, but also *Atrogin-1* and *MuRF-1* gene expression (Fig. 5). Within 6 hrs following stimulation of the denervated soleus muscle *Myog*, *Atrogin-1* and *MuRF-1* mRNAs are dramatically reduced and by 24–48 hrs of electrical stimulation these mRNAs approach or are below basal levels. These data suggest that all 3 of these mRNAs are regulated by muscle electrical activity and are consistent with the idea that Myog regulates *Atrogin-1* and *MuRF-1* gene expression.

Myog regulates *Atrogin-1* and *MuRF-1* gene expression in denervated muscle

To directly test the idea that Myog controls atrophy-related gene expression in denervated muscle, we compared *Atrogin-1* and *MuRF-1* mRNA expression in *Wt* and *Myog* null mice. We also assayed *FoxO3* expression in these mice because FoxO3 contributes to denervation-induced muscle atrophy [Mammucari et al., 2007; Sandri et al., 2006; Sandri et al., 2004; Zhao et al., 2007], at least in part, by stimulating *Atrogin-1* gene expression [Sandri et al., 2004]. Therefore Myog may act on *Atrogin-1* and *MuRF-1* gene expression directly or indirectly via regulated expression of *FoxO3*. To test these possibilities we compared denervation-dependent gene expression in *Wt* and *Myog* null mice. We chose 3 days post-denervation for these assays because this is when *Atrogin-1* RNA levels are reported to be highest [Sacheck et al., 2007]. Real-time PCR showed that muscle denervation induced *Atrogin-1* mRNA by about 5.5-fold, *MuRF1* mRNA by almost 4-fold, and *Myog* mRNA by about 27-fold (Fig. 6). Interestingly, these genes were not induced in *Myog* null mice (Fig. 6). In contrast, *FoxO3* mRNA expression does not appear to be significantly regulated by muscle denervation (Fig. 6). These data are consistent with the idea that Myog mediates denervation-dependent induction of *Atrogin-1* and *MuRF-1* gene expression.

Because *Atrogin-1* gene expression was more robustly regulated by muscle activity than *MuRF-1* gene expression, we focused on this gene to further examine its regulation by Myog. To investigate if Myog can induce *Atrogin-1* gene expression *in vivo*, we electroporated adult innervated soleus muscle with *pCS2:Myog* and *pCS2:EGFP* expression vectors. Twelve days following electroporation, soleus muscles were isolated, GFP-expressing fibers dissected and RNA isolated for analysis of *Myog*, *Atrogin-1* and *γ-actin* mRNA levels by Real-time PCR. This analysis showed that a Myog over-expression induced *Atrogin-1* mRNA levels (Fig. 7A). These results suggest that Myog may directly activate the *Atrogin-1* promoter. Indeed, inspection of the 3.5kb *Atrogin-1* promoter identified 8 putative Myog binding sites (E-boxes, CANNTG) (Fig. 7). Interestingly, 4 of these sites conform to previously identified Myog binding sites (CACCTG, CAGCTG) that have been shown to be necessary for denervation-dependent activation of the muscle-specific *nAChR* and *MuSK* promoters [Tang et al., 2006]. Co-transfection of HEK 293 cells with an *Atrogin-1:luciferase* expression vector and *pCS2-Myog* showed Myog regulates *Atrogin-1* promoter activity. In addition, a series of promoter deletions indicated reduced promoter activity in both HEK 293 cells over-expressing Myog (Fig. 7B) and in denervated soleus muscle (Fig. 7C) that presumably reflects the reduction in Myog binding sites. Deletion of distal E-boxes located between −1 and −3.5kb from the translation start site had a large consequence on the ability of Myog to activate *Atrogin-1* promoter activity in denervated muscle (Fig. 7C) and may suggest that these distal E-boxes play a more significant role than the more proximal E-boxes in denervation-dependent *Atrogin-1* gene activation. Taken together, these data are consistent with the idea that Myog mediates its effects on muscle atrophy by directly regulating *Atrogin-1* promoter activity.

Discussion

The main finding from this study is that Myog expression contributes to denervation-induced muscle atrophy. Myog is best known for its role in muscle fiber formation during early development where it is necessary for myoblast differentiation and fusion [Hasty et al., 1993; Venuti et al., 1995; Vivian et al., 1999]. Postnatally, Myog expression is suppressed by muscle innervation in an activity-dependent manner [Buonanno et al., 1992; Eftimie et al., 1991]. Denervation of adult muscle induces Myog expression where it plays an important role in mediating both denervation-dependent gene induction and suppression [Tang and Goldman, 2006; Tang et al., 2004; Tang et al., 2009; Tang et al., 2006]. Genes that are regulated, either directly or indirectly, by Myog include those involved in synapse formation, muscle fiber determination and muscle metabolism [Tang and Goldman, 2006; Tang et al., 2009].

We were intrigued by the large induction in *Atrogin-1* gene expression following muscle denervation [Sacheck et al., 2007] and tested the idea that denervation-dependent Myog expression mediated this induction. Indeed our data suggests that Myog regulates *Atrogin-1* gene expression in denervated muscle which, along with previously published data showing Atrogin-1 expression contributes to muscle atrophy [Bodine et al., 2001a], is consistent with the hypothesis that Myog contributes to denervation-induced muscle atrophy.

We took advantage of mice that conditionally express Myog to investigate its role in denervation-induced muscle atrophy. Previous studies had shown that Myog is necessary for muscle fiber formation during embryonic periods of development while loss of Myog postnatally has little consequence on muscle growth [Hasty et al., 1993; Knapp et al., 2006; Venuti et al., 1995; Vivian et al., 1999]. We deleted *Myog* in adult mice and found that these mice exhibited less denervation-induced muscle atrophy than *Wt* controls. This effect was most pronounced for the slow soleus muscle and unremarkable for the fast EDL muscle. This is not too surprising since previous studies have documented that slow muscle fibers are more prone to atrophy than fast muscle fibers [Grossman et al., 1998] and may suggest that Myog and its targets, such as *Atrogin-1*, are differentially regulated in fast and slow muscle fibers. Indeed basal Myog expression is known to be higher in soleus compared to EDL [Hughes et al., 1993; Voytik et al., 1993]. However, whether this basal expression contributes to the differential atrophy noted in soleus and EDL muscles is not clear.

We investigated if the protection against muscle atrophy is a result of increased satellite cell proliferation and fusion with existing muscle fibers in *Myog* knockout mice. Surprisingly we found that denervation-induced satellite cell proliferation is reduced in Myog knockout mice and therefore cannot account for the maintenance of muscle mass or cross sectional area in their denervated fibers. It has been previously suggested that contact between muscle and nerve, independent of muscle activity, is sufficient to suppress satellite cell proliferation [Hyatt et al., 2003]. Our data suggests that Myog may be a factor that mediates this effect of the nerve on muscle satellite cells.

Of the genes previously shown to participate in muscle atrophy, we identified *Atrogin-1* as a putative Myog target. Data supporting this idea include: 1) lack of *Atrogin-1* induction following muscle denervation in *Myog* knockout mice; 2) *Myog* over-expression in innervated muscle induced *Atrogin-1* gene expression; and 3) *Myog*-dependent and denervation-dependent activation of the *Atrogin-1* promoter in tissue culture cells and soleus muscle, respectively. Thus Myog appears to mediate its effect on muscle atrophy, at least in part, via activation of *Atrogin-1* gene expression. *MuRF-1* mRNA was also induced in denervated soleus muscle of *Wt* mice but not in *Myog* null mice which suggests Myog also contributes to muscle atrophy by controlling denervation-dependent induction of *MuRF-1*.

Previous studies have suggested that *Atrogin-1* and *MuRF-1* gene expression is regulated by the forkhead transcription factor, FoxO3 [Bodine et al., 2001b; Sandri et al., 2004]. FoxO3 activity is induced by the PI3K/AKT signaling cascade and inhibited by PGC-1α [Bodine et al., 2001b; Sandri et al., 2006; Sandri et al., 2004]. In addition, NF-kB signaling also impinges on muscle atrophy, at least in part, by increased expression of MuRF-1 [Cai et al., 2004; Mourkioti et al., 2006]. There are no studies linking denervation-dependent *Myog* gene expression to FoxO3 or NF-kB signaling pathway, suggesting that denervation-dependent *Myog* gene activation may be under the control of other signaling cascades.

The mechanism by which the *Myog* gene is activated in denervated muscle is of interest because it may represent a new target for reducing the detrimental consequences of muscle denervation following injury or disease. We and others have previously reported that denervation-dependent *Myog* gene induction is accompanied by translocation of HDAC4 to the nucleus and that HDAC4 expression is necessary for *Myog* gene expression [Cohen et al., 2007; Tang et al., 2009]. HDAC4 stimulates *Myog* gene expression by suppressing expression of the *Myog* gene transcriptional co-repressors, Dach2 and MITR [Cohen et al., 2007; Mejat et al., 2005; Tang and Goldman, 2006; Tang et al., 2009]. Myog also stimulates *HDAC4* gene expression, reinforcing the continued expression of these genes in denervated muscle [Tang et al., 2009]. Interestingly, while this manuscript was in preparation it was reported that not only Myog, but also HDAC4 and 5 contribute to denervation-induced muscle atrophy [Moresi et al., 2010]. This latter study also came to the conclusion that Myog mediates its effects on muscle atrophy by regulating *Atrogin-1* and *MuRF1* gene expression. The HDAC4/5-Dach2-Myog signaling cascade impinges on a large number of genes induced in denervated muscle that influence muscle fiber metabolism, synapse formation and atrophy and therefore represents a potential target for reducing the detrimental consequences of muscle atrophy following injury or disease. However, because inhibition of this signaling pathway would contribute to maintaining a pattern of gene expression more like innervated muscle and because innervated muscle is resistant to reinnervation, inhibition of this signaling pathway in denervated muscle may preserve muscle mass at the expense of enhancing muscle reinnervation.

Acknowledgments

Grant Sponsor: Muscular Dystrophy Association and the National Institutes of Health (NINDS 5 RO1 NS59848).

We thank Dr. William Klein (Univ. of Texas, MD Anderson Cancer Center) for providing conditional *Myog* knockout mice, Dr. Alfred Goldberg (Harvard Medical School) for sharing their *Atrogin-1* promoter: luciferase expression constructs, the contractility core in the Nathan Shock Center for Excellence in The Basic Biology of Aging at the University of Michigan and members of the Goldman lab for advice and encouragement during these studies.

References

Bodine SC, Latres E, Baumhueter S, Lai VK, Nunez L, Clarke BA, Poueymirou WT, Panaro FJ, Na E, Dharmarajan K, Pan ZQ, Valenzuela DM, DeChiara TM, Stitt TN, Yancopoulos GD, Glass DJ. Identification of ubiquitin ligases required for skeletal muscle atrophy. Science. 2001a; 294:1704–8. [PubMed: 11679633]

Bodine SC, Stitt TN, Gonzalez M, Kline WO, Stover GL, Bauerlein R, Zlotchenko E, Scrimgeour A, Lawrence JC, Glass DJ, Yancopoulos GD. Akt/mTOR pathway is a crucial regulator of skeletal muscle hypertrophy and can prevent muscle atrophy in vivo. Nat Cell Biol. 2001b; 3:1014–9. [PubMed: 11715023]

Brooks SV, Faulkner JA. Contractile properties of skeletal muscles from young, adult and aged mice. J Physiol. 1988; 404:71–82. [PubMed: 3253447]

Buonanno A, Apone L, Morasso MI, Beers R, Brenner HR, Eftimie R. The MyoD family of myogenic factors is regulated by electrical activity: isolation and characterization of a mouse Myf-5 cDNA. Nucleic Acids Res. 1992; 20:539–44. [PubMed: 1741288]

Cai D, Frantz JD, Tawa NE Jr, Melendez PA, Oh BC, Lidov HG, Hasselgren PO, Frontera WR, Lee J, Glass DJ, Shoelson SE. IKKbeta/NF-kappaB activation causes severe muscle wasting in mice. Cell. 2004; 119:285–98. [PubMed: 15479644]

Cao PR, Kim HJ, Lecker SH. Ubiquitin-protein ligases in muscle wasting. Int J Biochem Cell Biol. 2005; 37:2088–97. [PubMed: 16125112]

Cohen TJ, Waddell DS, Barrientos T, Lu Z, Feng G, Cox GA, Bodine SC, Yao TP. The histone deacetylase HDAC4 connects neural activity to muscle transcriptional reprogramming. J Biol Chem. 2007; 282:33752–9. [PubMed: 17873280]

Eftimie R, Brenner HR, Buonanno A. Myogenin and MyoD join a family of skeletal muscle genes regulated by electrical activity. Proc Natl Acad Sci U S A. 1991; 88:1349–53. [PubMed: 1705035]

Goldman D, Brenner HR, Heinemann S. Acetylcholine receptor alpha-, beta-, gamma-, and delta-subunit mRNA levels are regulated by muscle activity. Neuron. 1988; 1:329–33. [PubMed: 3272739]

Gomes MD, Lecker SH, Jagoe RT, Navon A, Goldberg AL. Atrogin-1, a muscle-specific F-box protein highly expressed during muscle atrophy. Proc Natl Acad Sci U S A. 2001; 98:14440–5. [PubMed: 11717410]

Grossman EJ, Roy RR, Talmadge RJ, Zhong H, Edgerton VR. Effects of inactivity on myosin heavy chain composition and size of rat soleus fibers. Muscle Nerve. 1998; 21:375–89. [PubMed: 9486867]

Hasty P, Bradley A, Morris JH, Edmondson DG, Venuti JM, Olson EN, Klein WH. Muscle deficiency and neonatal death in mice with a targeted mutation in the myogenin gene. Nature. 1993; 364:501–6. [PubMed: 8393145]

Hughes SM, Taylor JM, Tapscott SJ, Gurley CM, Carter WJ, Peterson CA. Selective accumulation of MyoD and myogenin mRNAs in fast and slow adult skeletal muscle is controlled by innervation and hormones. Development. 1993; 118:1137–47. [PubMed: 8269844]

Hyatt JP, Roy RR, Baldwin KM, Edgerton VR. Nerve activity-independent regulation of skeletal muscle atrophy: role of MyoD and myogenin in satellite cells and myonuclei. Am J Physiol Cell Physiol. 2003; 285:C1161–73. [PubMed: 12839833]

Knapp JR, Davie JK, Myer A, Meadows E, Olson EN, Klein WH. Loss of myogenin in postnatal life leads to normal skeletal muscle but reduced body size. Development. 2006; 133:601–10. [PubMed: 16407395]

Kostrominova TY, Macpherson PC, Carlson BM, Goldman D. Regulation of myogenin protein expression in denervated muscles from young and old rats. Am J Physiol Regul Integr Comp Physiol. 2000; 279:R179–88. [PubMed: 10896880]

Mammucari C, Milan G, Romanello V, Masiero E, Rudolf R, Del Piccolo P, Burden SJ, Di Lisi R, Sandri C, Zhao J, Goldberg AL, Schiaffino S, Sandri M. FoxO3 controls autophagy in skeletal muscle in vivo. Cell Metab. 2007; 6:458–71. [PubMed: 18054315]

Mejat A, Ramond F, Bassel-Duby R, Khochbin S, Olson EN, Schaeffer L. Histone deacetylase 9 couples neuronal activity to muscle chromatin acetylation and gene expression. Nat Neurosci. 2005; 8:313–21. [PubMed: 15711539]

Mejat A, Ravel-Chapuis A, Vandromme M, Schaeffer L. Synapse-specific gene expression at the neuromuscular junction. Ann N Y Acad Sci. 2003; 998:53–65. [PubMed: 14592863]

Mittal A, Bhatnagar S, Kumar A, Lach-Trifilieff E, Wauters S, Li H, Makonchuk DY, Glass DJ. The TWEAK-Fn14 system is a critical regulator of denervation-induced skeletal muscle atrophy in mice. J Cell Biol. 2010; 188:833–49. [PubMed: 20308426]

Moresi V, Williams AH, Meadows E, Flynn JM, Potthoff MJ, McAnally J, Shelton JM, Backs J, Klein WH, Richardson JA, Bassel-Duby R, Olson EN. Myogenin and class II HDACs control neurogenic muscle atrophy by inducing E3 ubiquitin ligases. Cell. 2010; 143:35–45. [PubMed: 20887891]

Mourkioti F, Kratsios P, Luedde T, Song YH, Delafontaine P, Adami R, Parente V, Bottinelli R, Pasparakis M, Rosenthal N. Targeted ablation of IKK2 improves skeletal muscle strength,

maintains mass, and promotes regeneration. J Clin Invest. 2006; 116:2945–54. [PubMed: 17080195]

Ramachandran R, Fausett BV, Goldman D. Ascl1a regulates Muller glia dedifferentiation and retinal regeneration through a Lin-28-dependent, let-7 microRNA signalling pathway. Nat Cell Biol. 2010; 12:1101–7. [PubMed: 20935637]

Rommel C, Bodine SC, Clarke BA, Rossman R, Nunez L, Stitt TN, Yancopoulos GD, Glass DJ. Mediation of IGF-1-induced skeletal myotube hypertrophy by PI(3)K/Akt/mTOR and PI(3)K/Akt/GSK3 pathways. Nat Cell Biol. 2001; 3:1009–13. [PubMed: 11715022]

Sacheck JM, Hyatt JP, Raffaello A, Jagoe RT, Roy RR, Edgerton VR, Lecker SH, Goldberg AL. Rapid disuse and denervation atrophy involve transcriptional changes similar to those of muscle wasting during systemic diseases. FASEB J. 2007; 21:140–55. [PubMed: 17116744]

Sandri M, Lin J, Handschin C, Yang W, Arany ZP, Lecker SH, Goldberg AL, Spiegelman BM. PGC-1alpha protects skeletal muscle from atrophy by suppressing FoxO3 action and atrophy-specific gene transcription. Proc Natl Acad Sci U S A. 2006; 103:16260–5. [PubMed: 17053067]

Sandri M, Sandri C, Gilbert A, Skurk C, Calabria E, Picard A, Walsh K, Schiaffino S, Lecker SH, Goldberg AL. Foxo transcription factors induce the atrophy-related ubiquitin ligase atrogin-1 and cause skeletal muscle atrophy. Cell. 2004; 117:399–412. [PubMed: 15109499]

Stitt TN, Drujan D, Clarke BA, Panaro F, Timofeyva Y, Kline WO, Gonzalez M, Yancopoulos GD, Glass DJ. The IGF-1/PI3K/Akt pathway prevents expression of muscle atrophy-induced ubiquitin ligases by inhibiting FOXO transcription factors. Mol Cell. 2004; 14:395–403. [PubMed: 15125842]

Tang H, Goldman D. Activity-dependent gene regulation in skeletal muscle is mediated by a histone deacetylase (HDAC)-Dach2-myogenin signal transduction cascade. Proc Natl Acad Sci U S A. 2006; 103:16977–82. [PubMed: 17075071]

Tang H, Macpherson P, Argetsinger LS, Cieslak D, Suhr ST, Carter-Su C, Goldman D. CaM kinase II-dependent phosphorylation of myogenin contributes to activity-dependent suppression of nAChR gene expression in developing rat myotubes. Cell Signal. 2004; 16:551–63. [PubMed: 14751541]

Tang H, Macpherson P, Marvin M, Meadows E, Klein WH, Yang XJ, Goldman D. A histone deacetylase 4/myogenin positive feedback loop coordinates denervation-dependent gene induction and suppression. Mol Biol Cell. 2009; 20:1120–31. [PubMed: 19109424]

Tang H, Sun Z, Goldman D. CaM kinase II-dependent suppression of nicotinic acetylcholine receptor delta-subunit promoter activity. J Biol Chem. 2001; 276:26057–65. [PubMed: 11350961]

Tang H, Veldman MB, Goldman D. Characterization of a muscle-specific enhancer in human MuSK promoter reveals the essential role of myogenin in controlling activity-dependent gene regulation. J Biol Chem. 2006; 281:3943–53. [PubMed: 16361705]

Ventadour S, Attaix D. Mechanisms of skeletal muscle atrophy. Curr Opin Rheumatol. 2006; 18:631–5. [PubMed: 17053511]

Venuti JM, Morris JH, Vivian JL, Olson EN, Klein WH. Myogenin is required for late but not early aspects of myogenesis during mouse development. J Cell Biol. 1995; 128:563–76. [PubMed: 7532173]

Vivian JL, Gan L, Olson EN, Klein WH. A hypomorphic myogenin allele reveals distinct myogenin expression levels required for viability, skeletal muscle development, and sternum formation. Dev Biol. 1999; 208:44–55. [PubMed: 10075840]

Voytik SL, Przyborski M, Badylak SF, Konieczny SF. Differential expression of muscle regulatory factor genes in normal and denervated adult rat hindlimb muscles. Dev Dyn. 1993; 198:214–24. [PubMed: 8136525]

Zhao J, Brault JJ, Schild A, Cao P, Sandri M, Schiaffino S, Lecker SH, Goldberg AL. FoxO3 coordinately activates protein degradation by the autophagic/lysosomal and proteasomal pathways in atrophying muscle cells. Cell Metab. 2007; 6:472–83. [PubMed: 18054316]

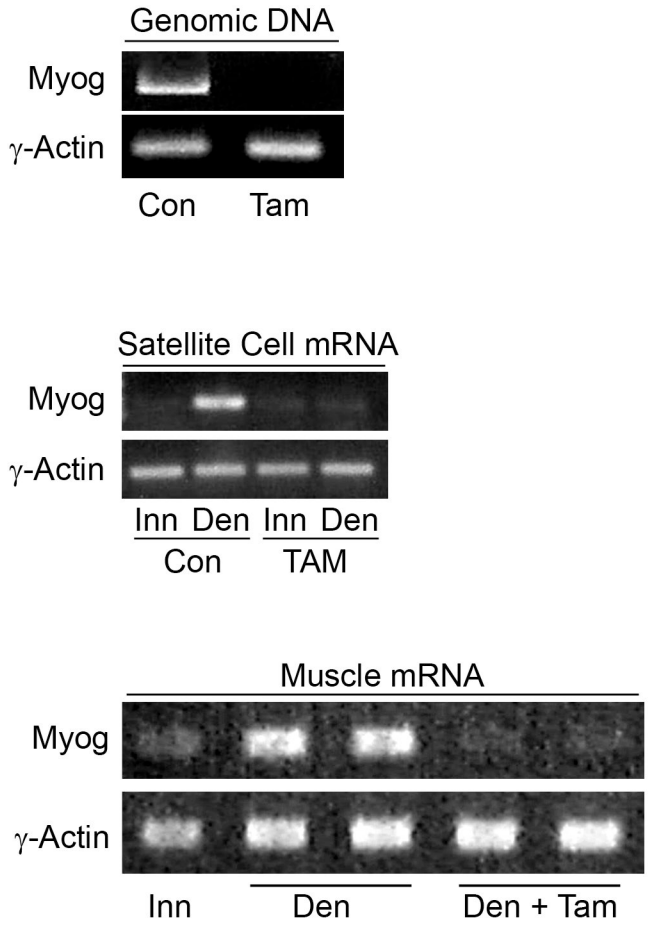

Figure 1. Conditional ablation of *Myog* gene expression

Myog$^{flox/flox}$;*CAGG-CreER*^{TM} mice were injected with vehicle (Con) or tamoxifen (Tam) for 5 days. Left lower hindlimb muscles were denervated by sciatic nerve transection and 3–7 days later innervated and denervated muscles were dissected. Genomic DNA was isolated for PCR amplification of exon 1 from the *Myog* gene (top panel). RNA was isolated from satellite cells (middle panel) or from muscle (bottom panel). Shown are ethidium bromide stained gels used to resolve the amplified gene products. Note that tamoxifen treatment prevented amplification of genomic DNA containing exon 1 of the Myog gene (top panel) and also prevented denervation-dependent *Myog* mRNA induction (Den + Tam) (middle and bottom panels), while animals that did not receive tamoxifen showed a large increase in *Myog* mRNA expression following muscle denervation (Compare Inn and Den lanes in the middle and bottom panels). Experiments were done in duplicate.

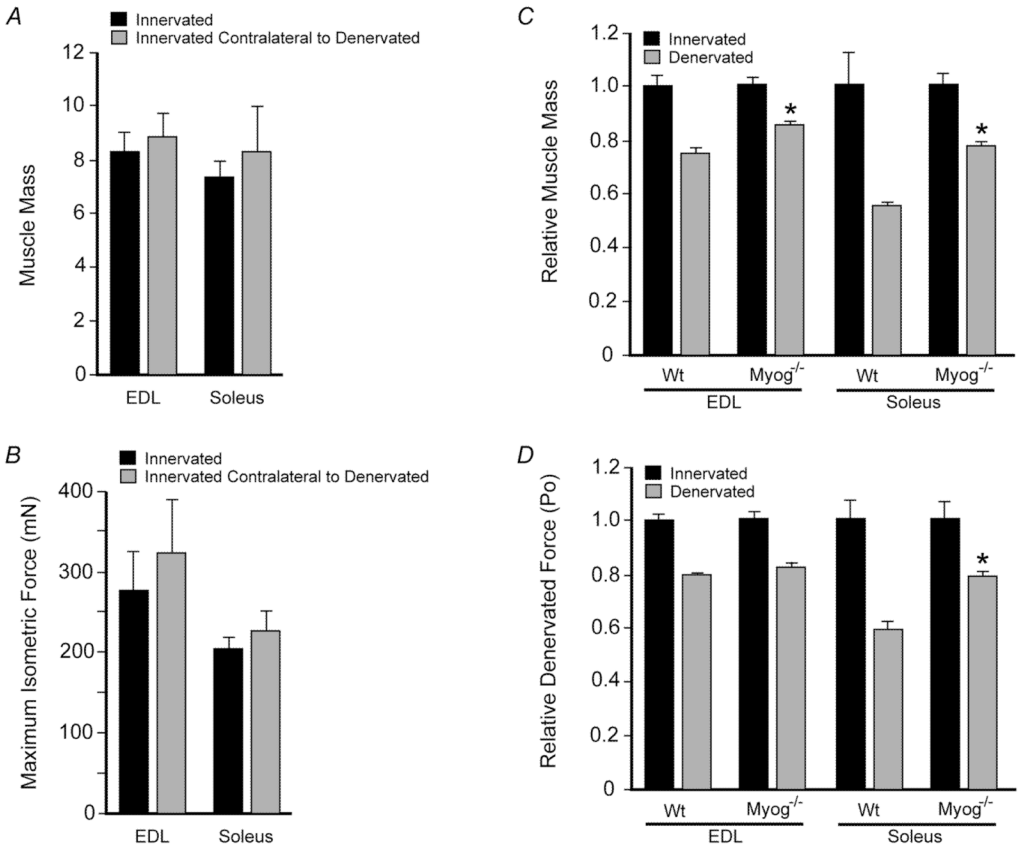

Figure 2. *Myog* deletion inhibits denervation-dependent reductions in muscle mass and force

The left lower hindlimb muscles of *Wt* or *Myog* null (Myog$^{-/-}$) mice were denervated for 14 days. Innervated and denervated EDL and soleus muscles were then dissected and muscle mass (A) and force (B) assayed. Reported is the denervated mass and force relative to the contralateral innervated muscle. Note that *Myog* deletion attenuates denervation-dependent loss in muscle mass and force, especially for the soleus muscle. Error bars are standard error of the mean (n=4).

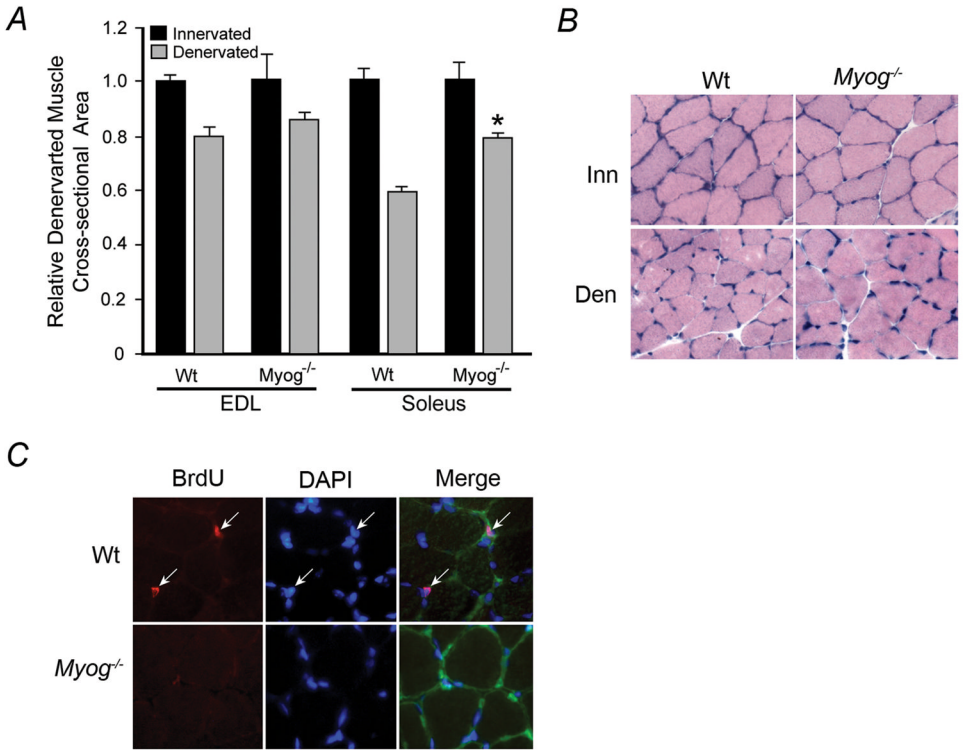

Figure 3. *Myog* deletion attenuates denervation-dependent reductions in muscle cross sectional area

The left lower hindlimb muscles of *Wt* or *Myog* null (Myog$^{-/-}$) mice were denervated for 14 days. Innervated and denervated EDL and soleus muscles were then dissected and muscle cross sectional areas measured. (A) Cross sectional areas relative to the innervated control are reported. Experiments were done in triplicate and 3 random areas from each muscle were sampled for fiber cross sectional areas. Error bars are standard error of the mean. (B) Typical cross section through an innervated and denervated soleus muscle from *Wt* and *Myog* null (Myog$^{-/-}$) mice. Note reduced denervation-dependent soleus muscle atrophy in Myog$^{-/-}$ mice. (C) Adult hind limb muscles were denervated and 5 days later BrdU was injected (once daily) into animals for the next 8 days. Soleus muscles were collected and stained for laminin (green) to identify the extracellular matrix, BrdU (red) to identify dividing cells and DAPI (blue) to visualize nuclei.

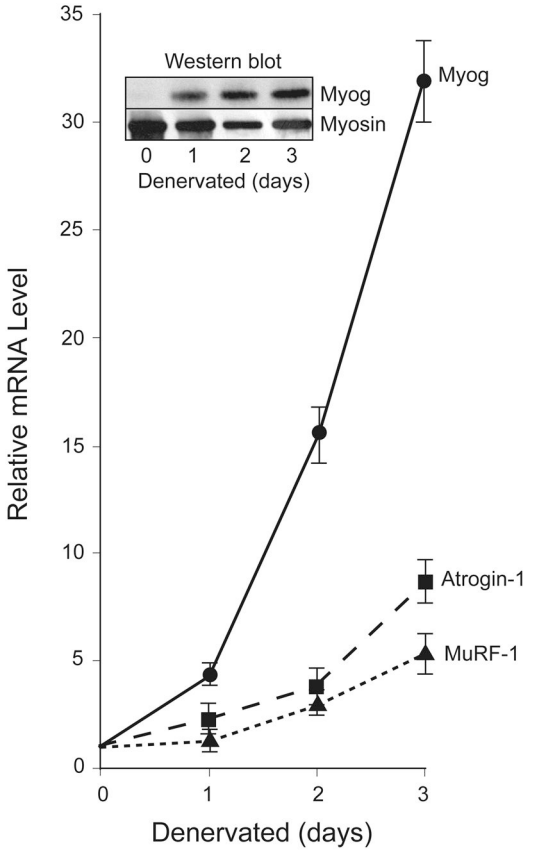

Figure 4. Denervation-dependent regulation of *Myog*, *Atrogin-1* and *MuRF-1* gene expression

Lower hindlimb muscles of adult mice were denervated for the indicated times. Real-time PCR was used to quantify *Myog*, *Atrogin-1*, *MuRF-1* and *Actin* mRNA levels. RNA levels were normalized to *Actin* RNA levels and then normalized to innervated RNA levels. Western blots were used to assay denervation-dependent Myog protein induction. Myosin protein levels were used to reveal differences in the amount of protein loaded onto the gel. Error bars are standard error of the mean (n=3).

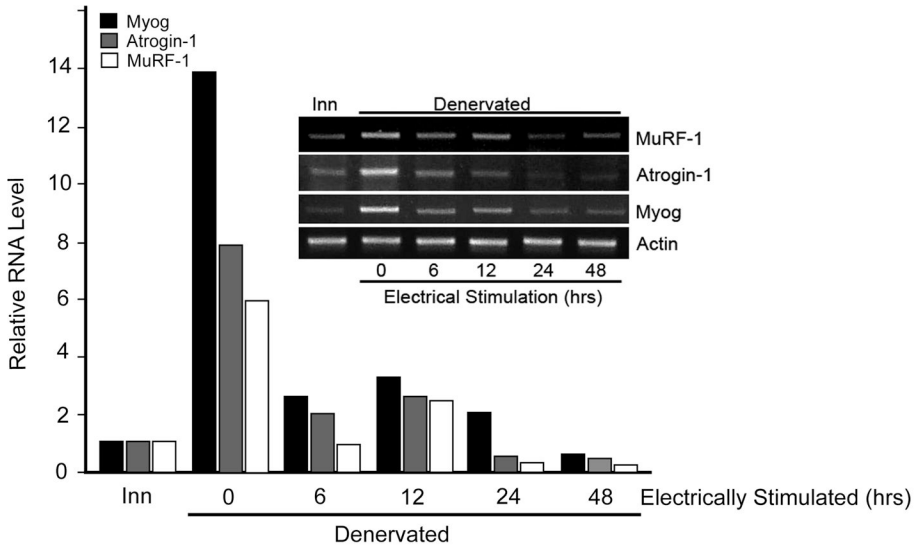

Figure 5. Direct electrical stimulation of denervated soleus muscle suppresses denervation-dependent induction of *Myog*, *Atrogin-1* and *MuRF-1* mRNAs

Lower hind limbs of adult rats were bilaterally denervated and stimulating electrodes were implanted into one hind limb. Denervated soleus muscles were electrically stimulated for 0–48 hrs. RNA was isolated from innervated, 3-day denervated and 3-day denervated/stimulated soleus muscle and assayed by RT-PCR (representative ethidium bromide stained agarose gel is shown) and Real-time PCR (graph). Note that direct electrical stimulation of soleus muscle rapidly suppressed denervation-dependent *Myog*, *Atrogin-1* and *MuRF-1* gene expression. Experiments were repeated twice with almost identical results.

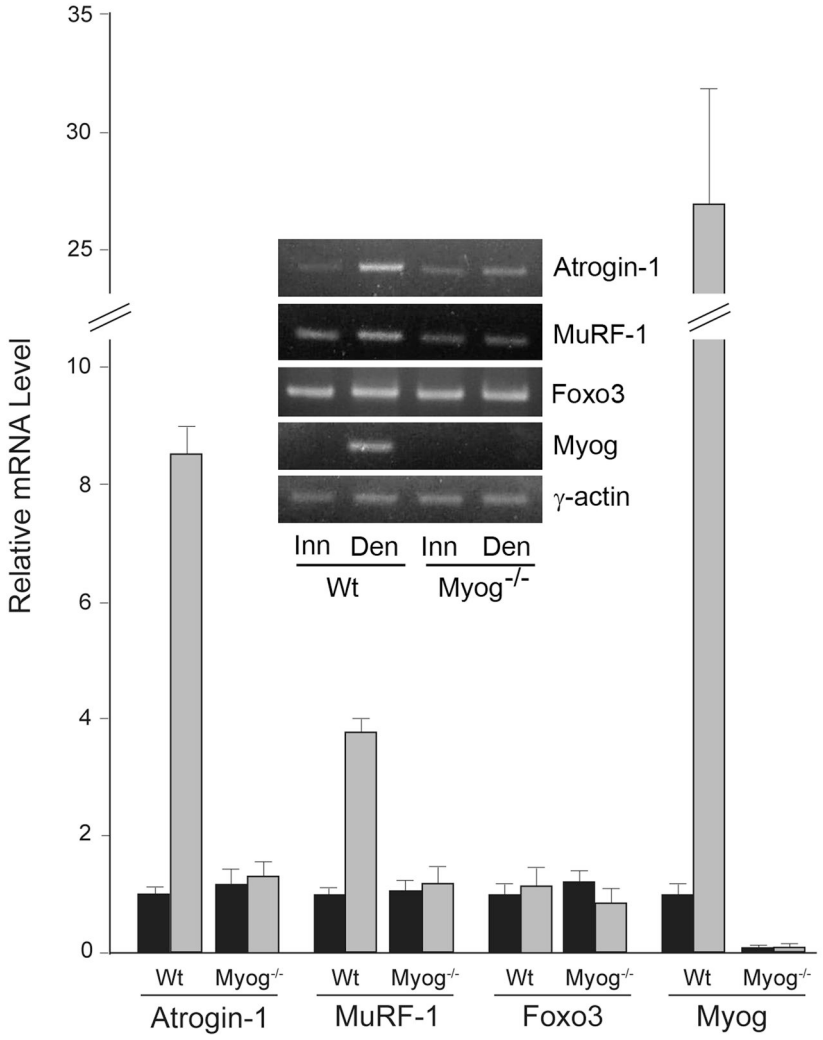

Figure 6. Regulation of atrophy gene expression in *Wt* and *Myog*$^{-/-}$ mice

The left lower hind limb muscles of *Wt* or *Myog* null (Myog$^{-/-}$) mice were denervated for 3 days. Innervated and denervated soleus muscles were then dissected and RNA extracted for RT-PCR. Ethidium bromide stained gel shows the relative transcript levels. Real-time PCR was used to quantify these levels which are shown in the graph. Note that *Myog* deletion blocks denervation-dependent induction of *Atrogin-1*, *MuRF-1* and *Myog* mRNA expression while *FoxO3* mRNA expression is slightly increased in following muscle denervation. Error bars are standard error of the mean (n=3).

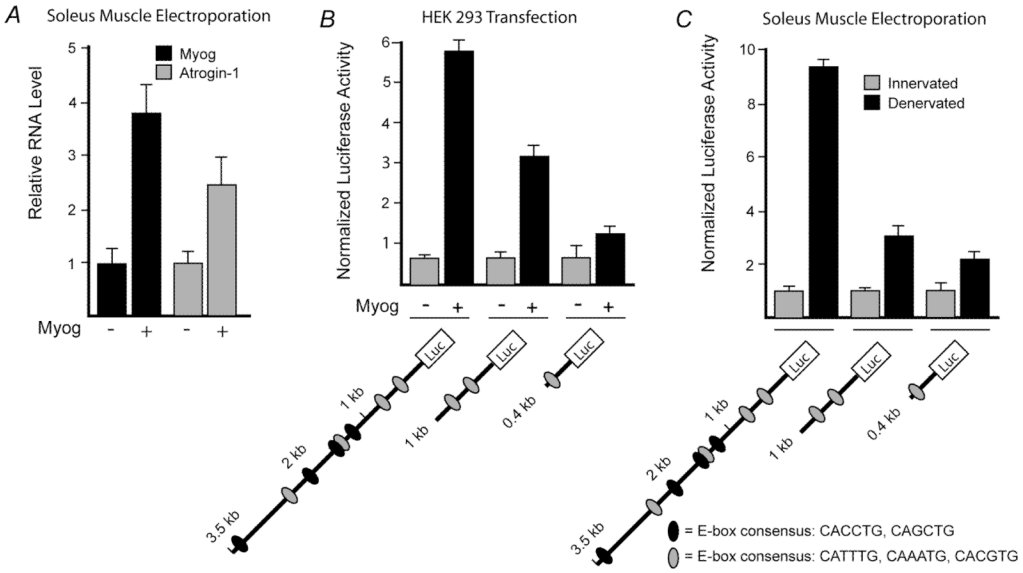

Figure 7. *Myog* regulates *Atrogin-1* gene expression and *Atrogin-1* promoter activity

(A) *pCS2:Myog* and *pCS2:EGFP* expression vectors were electroporated into innervated soleus muscle of *Wt* animals. Twelve days later soleus muscles were harvested and GFP-expressing fibers dissected for RNA analysis. Real-time PCR was used to quantify *Myog* and *Atrogin-1* mRNA levels. Note *Myog* overexpression induced *Atrogin-1* expression. Error bars are standard error of the mean (n=3). (B) *Atrogin-1* promoter activity is regulated by Myog overexpression. HEK 293 cells were co-transfected with an *Atrogin-1:luciferase* reporter vector harboring various lengths of the *Atrogin-1* promoter upstream of the firefly *luciferase* sequence and a normalization vector *ubC:Renilla luciferase* that harbors the human *Ubiquitin* promoter upstream of the *Renilla luciferase* sequence, with and without *pCS2:Myog* which allows for overexpression of Myog from the simian *CMV* promoter. (C) The soleus muscle of adult mice was electroporated with *Atrogin-1:luciferase* reporter plasmid[Sandri et al., 2004], *pCS2:EGFP* to identify electroporated fibers and *ubC:Renilla* luciferase for normalization. 12 days post-electroporation the left hindlimb muscle was denervated for 3 days and then GFP^+ fibers were dissected from innervated and denervated electroporated muscles for luciferase assays. Black ovals in the promoter cartoon indicate E-boxes (CANNTG) that conform to the consensus Myog binding E-box, while grey ovals represent E-boxes that do not conform to this consensus sequence. Note the stimulation of *Atrogin-1* promoter activity by Myog overexpression and muscle denervation and that as one deletes promoter sequences harboring E-boxes, Myog-dependent and denervation-dependent *Atrogin-1* promoter activation is reduced. Experiments were performed in triplicate. Error bars are standard error of the mean (n=3).